

Supplementary to

Rashba Torque Driven Domain Wall Motion in Magnetic Helices

Oleksandr V. Pylypovskiy^{1,*}, Denis D. Sheka^{1,†}, Volodymyr P. Kravchuk^{2,‡}, Kostiantyn V. Yershov^{2,3,§}, Denys Makarov^{4,5,¶}, and Yuri Gaididei^{2,**}

¹Taras Shevchenko National University of Kyiv, 01601 Kyiv, Ukraine

²Bogolyubov Institute for Theoretical Physics of the National Academy of Sciences of Ukraine, 03680 Kyiv, Ukraine

³National University of “Kyiv-Mohyla Academy”, 04655 Kyiv, Ukraine

⁴Helmholtz-Zentrum Dresden-Rossendorf e. V., Institute of Ion Beam Physics and Materials Research, 01328 Dresden, Germany

⁵Institute for Integrative Nanosciences, IFW Dresden, 01069 Dresden, Germany

*engraver@univ.net.ua

†sheka@univ.net.ua

‡vkravchuk@bitp.kiev.ua

§yershov@bitp.kiev.ua

¶d.makarov@hzdr.de

**ybg@bitp.kiev.ua

ABSTRACT

The supplementary information provides details on analytical calculations of main aspect of the magnetization statics and dynamics of the transversal domain wall in a helix wire.

1 The model

Let us consider a curvilinear magnetic wire, which can be modelled by the 3D curved $\boldsymbol{\gamma} \subset \mathbb{R}^3$. We describe the magnetic properties of the wire using assumptions of classical ferromagnet with uniaxial anisotropy directed along the wire. The easy-tangential anisotropy in a curved magnet is spatially dependent. In order to describe the magnetization distribution in such systems it is convenient to use a curvilinear Frenet–Serret (TNB) parametrization of the curve $\boldsymbol{\gamma}$:

$$\mathbf{e}_T = \partial_s \boldsymbol{\gamma}, \quad \mathbf{e}_N = \frac{\partial_s \mathbf{e}_T}{|\partial_s \mathbf{e}_T|}, \quad \mathbf{e}_B = \mathbf{e}_T \times \mathbf{e}_N$$

with \mathbf{e}_T being the tangent, \mathbf{e}_N being the normal, and \mathbf{e}_B being the binormal to $\boldsymbol{\gamma}$ and s being the arc length. In particular, we use TNB parametrization of the magnetization unit vector,

$$\mathbf{m} = (m_T, m_N, m_B)^T \tag{S1}$$

with the curvilinear components m_α . Here and below Greek indices α, β numerate curvilinear coordinates (TNB-coordinates) and curvilinear components of vector fields. For an arbitrary thin wire the energy can be presented as follows¹

$$\begin{aligned} E &= K^{\text{eff}} S \int \mathcal{E} ds, \quad \mathcal{E} = \mathcal{E}_{\text{ex}} + \mathcal{E}_{\text{an}}, \\ \mathcal{E}_{\text{ex}} &= \mathcal{E}_{\text{ex}}^0 + \mathcal{E}_{\text{ex}}^D + \mathcal{E}_{\text{ex}}^A, \quad \mathcal{E}_{\text{ex}}^0 = |\mathbf{m}'|^2, \\ \mathcal{E}_{\text{ex}}^D &= \mathcal{F}_{\alpha\beta} (m_\alpha m'_\beta - m'_\alpha m_\beta), \quad \mathcal{E}_{\text{ex}}^A = \mathcal{H}_{\alpha\beta} m_\alpha m_\beta, \\ \mathcal{E}_{\text{an}} &= -m_T^2, \end{aligned} \tag{S2}$$

where the Einstein notation is used for summation, $K^{\text{eff}} = K + \pi M_s^2$, where the positive parameter K is a magnetocrystalline anisotropy constant of easy-tangential type, the term πM_s^2 comes from the magnetostatic contribution^{2–4} and S is the cross-section area. Here and below the prime denotes the derivative with respect to the dimensionless coordinate $u = s/\ell$ with

$\ell = \sqrt{A/K^{\text{eff}}}$ being a magnetic length (A is an exchange constant). The first term in the exchange energy $\mathcal{E}_{\text{ex}}^0$ describes the common isotropic part of exchange expression which has formally the same form as for the straight wire. The second term $\mathcal{E}_{\text{ex}}^{\text{D}}$ in the exchange energy functional is a curvature induced effective Dzyaloshinskii-Moriya interaction (DMI), which is linear with respect to curvature and torsion. The tensor of coefficients of such interaction is the dimensionless Frenet-Serret tensor¹

$$\|\mathcal{F}_{\alpha\beta}\| = \begin{pmatrix} 0 & \varkappa & 0 \\ -\varkappa & 0 & \sigma \\ 0 & -\sigma & 0 \end{pmatrix}.$$

Here $\varkappa = \kappa\ell$ and $\sigma = \tau\ell$ are the dimensionless curvature and torsion, respectively, with κ being the curvature and τ being the torsion. The term $\mathcal{E}_{\text{ex}}^{\text{A}}$ describes an effective anisotropy interaction, where the components of the tensor $\mathcal{K}_{\alpha\beta} = \mathcal{F}_{\alpha\nu}\mathcal{F}_{\beta\nu}$ are bilinear with respect to the curvature and the torsion,

$$\|\mathcal{K}_{\alpha\beta}\| = \begin{pmatrix} \varkappa^2 & 0 & -\varkappa\sigma \\ 0 & \varkappa^2 + \sigma^2 & 0 \\ -\varkappa\sigma & 0 & \sigma^2 \end{pmatrix}.$$

The energy of effective anisotropy

$$\mathcal{E}_{\text{eff}}^{\text{A}} = \mathcal{E}_{\text{an}} + \mathcal{E}_{\text{ex}}^{\text{A}} = \mathcal{K}_{\alpha\beta}^{\text{eff}} m_{\alpha} m_{\beta}, \quad \mathcal{K}_{\alpha\beta}^{\text{eff}} = \mathcal{K}_{\alpha\beta} - \delta_{\alpha,1} \delta_{\beta,1}$$

has a form, typical for biaxial magnets. The tensor of effective anisotropy coefficients $\mathcal{K}_{\alpha\beta}^{\text{eff}}$ has non-diagonal components. This means that the homogeneous magnetization structure is not oriented along the TNB basis. One can easily diagonalize it, by using a unitary transformation (rotation in a local rectifying plane) of the vector \mathbf{m} (S1)

$$\mathbf{m} = U \tilde{\mathbf{m}}, \quad \tilde{\mathbf{m}} = U^{-1} \mathbf{m}, \quad \tilde{\mathbf{m}} = (m_1, m_2, m_3)^T \quad U = \begin{pmatrix} \cos \psi & 0 & -\sin \psi \\ 0 & 1 & 0 \\ \sin \psi & 0 & \cos \psi \end{pmatrix}.$$

By choosing the rotation angle ψ as follows

$$\psi = \arctan \frac{\sigma \varkappa}{\mathcal{K}_0}, \quad \mathcal{K}_0 = \frac{1 + \sigma^2 - \varkappa^2 + \mathcal{K}_1}{2}, \quad \mathcal{K}_1 = \sqrt{(1 - \varkappa^2 + \sigma^2)^2 + 4\varkappa^2 \sigma^2}, \quad (\text{S3})$$

one can reduce the anisotropy energy $\mathcal{E}_{\text{eff}}^{\text{A}}$ to the form

$$\mathcal{E}_{\text{eff}}^{\text{A}} = -\mathcal{K}_1 m_1^2 + \mathcal{K}_2 m_2^2, \quad \mathcal{K}_2 = \frac{1 + \varkappa^2 + \sigma^2 - \mathcal{K}_1}{2} = \frac{2\varkappa^2}{1 + \varkappa^2 + \sigma^2 + \mathcal{K}_1}. \quad (\text{S4})$$

Here the coefficient \mathcal{K}_1 characterizes the strength of the effective easy-axis anisotropy while \mathcal{K}_2 gives the strength of the effective easy-surface anisotropy. The direction of effective easy axis is determined by \mathbf{e}_1 and the hard axis by \mathbf{e}_2 :

$$\mathbf{e}_1 = \mathbf{e}_T \cos \psi + \mathbf{e}_B \sin \psi, \quad \mathbf{e}_3 = -\mathbf{e}_T \sin \psi + \mathbf{e}_B \cos \psi.$$

One has to note that for any finite ψ the effective anisotropy direction \mathbf{e}_1 deviates from the magnetic anisotropy direction \mathbf{e}_T . Note that such a deviation vanishes for wires with zero torsion ($\sigma = 0$).

Apart from effective anisotropy, the curvature and torsion show up in the effective DMI, see Eq. (S2). In the new frame of reference (ψ -frame) the effective Dzyaloshinskii energy reads¹

$$\begin{aligned} \mathcal{E}_{\text{ex}}^{\text{D}} &= \mathcal{D}_1 (m_2 m'_3 - m_3 m'_2) + \mathcal{D}_2 (m_1 m'_2 - m_2 m'_1), \\ \mathcal{D}_1 &= 2\sigma \cos \psi + 2\varkappa \sin \psi = 2\sigma \frac{\mathcal{K}_0 + \varkappa^2}{\sqrt{\mathcal{K}_0^2 + \sigma^2 \varkappa^2}}, \quad \mathcal{D}_2 = 2\varkappa \cos \psi - 2\sigma \sin \psi = 2\varkappa \frac{\mathcal{K}_0 - \sigma^2}{\sqrt{\mathcal{K}_0^2 + \sigma^2 \varkappa^2}}. \end{aligned} \quad (\text{S5})$$

Finally we get the energy in the following form of Eq. (2) of the manuscript

$$\mathcal{E} = \underbrace{|\mathbf{m}'|^2}_{\text{isotropic exchange}} \underbrace{-\mathcal{K}_1 m_1^2 + \mathcal{K}_2 m_2^2}_{\text{effective anisotropy}} + \underbrace{\mathcal{D}_1 (m_2 m'_3 - m_3 m'_2) + \mathcal{D}_2 (m_1 m'_2 - m_2 m'_1)}_{\text{effective DMI}}. \quad (\text{2})$$

¹In the current analysis we suppose the spatio independence of the curvature and torsion (which is adequate for the helix geometry), hence $\varkappa' = \sigma' = 0$.

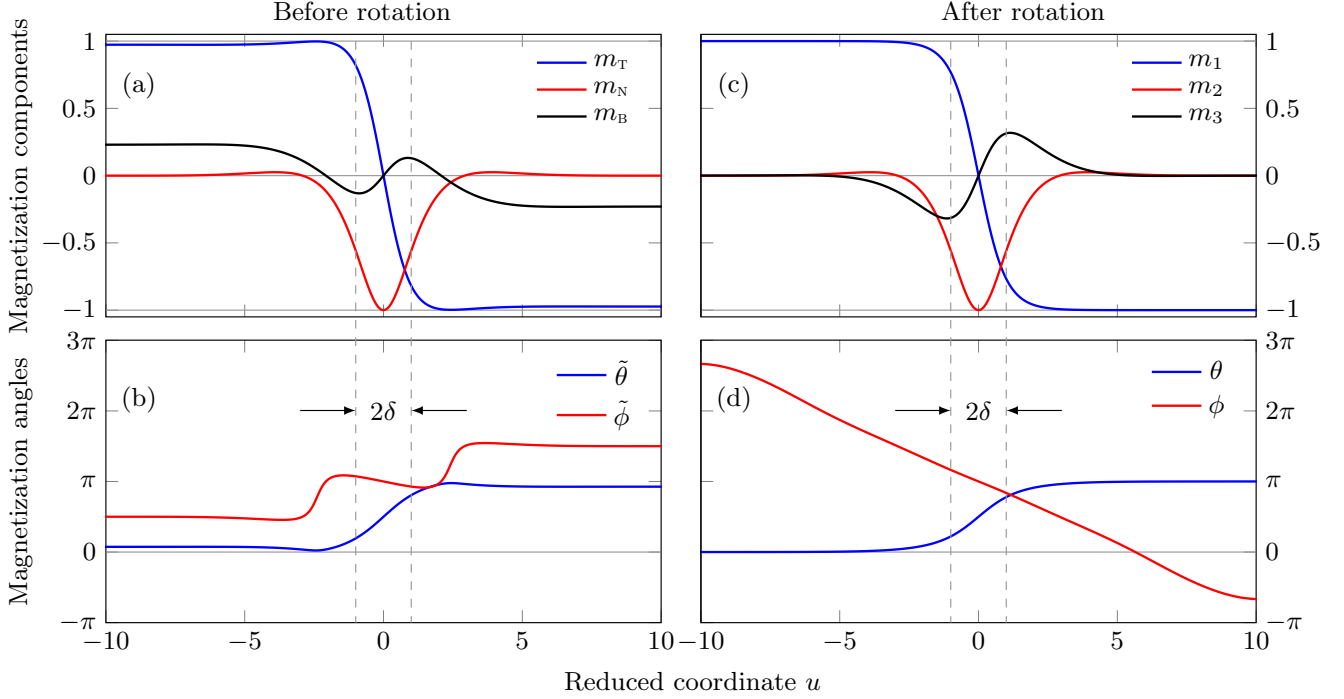


Figure S1. Comparison of the domain wall view in the TNB and the rotated reference frame (SLaSi simulations for the head-to-head domain wall): magnetization components $m_{T,N,B}$ and angles $\tilde{\theta} = \arccos m_T$, $\tilde{\phi} = \arctan m_B/m_N$. Right column: the same in the ψ -frame. Parameters: $\varkappa = 0.1$, $\sigma = 0.5$, $\ell = 15a$ with a being a lattice constant. Separate points are not shown due to their high density on the plots.

The dynamics of magnetization is described by the Landau–Lifshitz equations for the normalized magnetization \mathbf{m} . Using the angular parametrization,

$$\mathbf{m} = \cos \theta \mathbf{e}_1 + \sin \theta \cos \phi \mathbf{e}_2 + \sin \theta \sin \phi \mathbf{e}_3,$$

these equations can be derived from the Lagrangian

$$L = K^{\text{eff}} S \ell \int \mathcal{L} du, \quad \mathcal{L} = \mathcal{G} - \mathcal{E}, \quad \mathcal{G} = -\cos \theta \dot{\phi}, \quad (S6)$$

$$\mathcal{E} = \theta'^2 + \sin^2 \theta \phi'^2 - \mathcal{K}_1 \cos^2 \theta + \mathcal{K}_2 \sin^2 \theta \cos^2 \phi + \mathcal{D}_1 \sin^2 \theta \phi' + 2\mathcal{D}_2 \sin^2 \theta \cos \phi \theta'$$

and the dissipative function

$$F = K^{\text{eff}} S \ell \int \mathcal{F} du, \quad \mathcal{F} = \frac{\eta}{2} (\dot{\theta}^2 + \sin^2 \theta \dot{\phi}^2).$$

Here and below the overdot indicates derivative with respect to the rescaled time $\bar{t} = \omega_0 t$ and $\omega_0 = \gamma_e K^{\text{eff}} / M_s$.

2 Static Domain Wall

In the case of small enough curvature ($\varkappa \ll 1$) a static domain wall in the helix wire is well described by the expression (3) of the manuscript

$$\cos \theta^{\text{dw}}(u) = -p \tanh \frac{u}{\delta}, \quad \phi^{\text{dw}}(u) = \Phi - \Upsilon u, \quad (3)$$

where $p = \pm 1$ is a domain wall topological charge.

One can determine the magnetochirality, *i. e.* the chirality of the magnetization structure using the Lifshitz invariant

$$\mathcal{C} = \text{sgn} \int_{-\infty}^{\infty} (m_2 m_3' - m_3 m_2') du. \quad (S7)$$

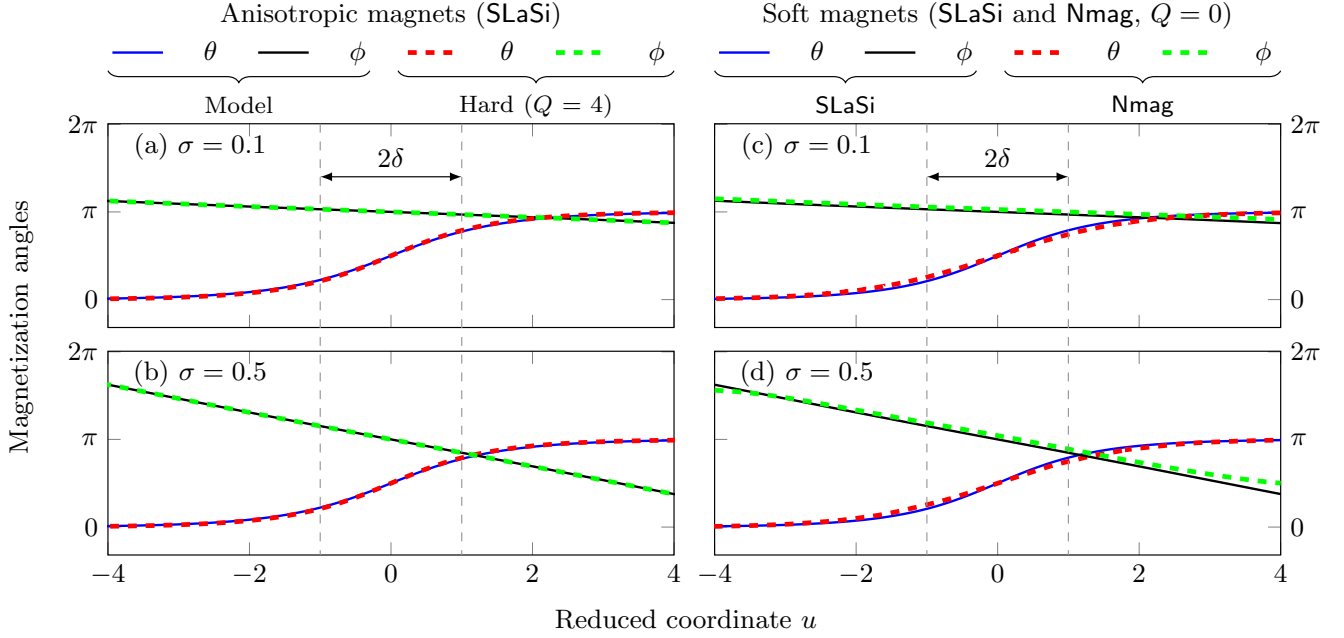


Figure S2. Influence of magnetostatics on the static domain wall: Magnetization angles in the ψ -frame for the head-to-head domain wall for $\varkappa = 0.1$ and different σ . Simulations without magnetostatics (model, solid lines) and of magnetically hard magnets ($Q = 4$, dashed lines) for $\sigma = 0.1$ (a) and $\sigma = 0.5$ (b), spin-lattice simulations in SLaSi. Simulations of magnetically soft magnets ($Q = 0$), spin-lattice simulations in SLaSi (solid lines) and micromagnetic simulations in Nmag (dashed lines) for $\sigma = 0.1$ (a) and $\sigma = 0.5$ (b). Magnetic parameters correspond to the magnetic length $\ell = 15a$. Rotation angle ψ_{sim} is determined from simulations for all curves where magnetostatics is taken into account [$|\psi - \psi_{\text{sim}}| < 0.004$, where ψ is determined by Eq. (S3)].

For the domain wall (S3) one gets $\mathcal{C} = -\text{sgn } Y$.

Let us compare the magnetization distribution in ψ -frame [Eq. (S3)] with the magnetization distribution in the TNB reference frame which are connected by the following relations:

$$m_T = m_1 \cos \psi - m_3 \sin \psi, \quad m_N = m_2, \quad m_B = m_1 \sin \psi + m_3 \cos \psi,$$

or, in the angular parametrization,

$$\cos \tilde{\theta} = m_T = \cos \theta \cos \psi - \sin \theta \sin \phi \sin \psi, \quad \tan \tilde{\phi} = \frac{m_B}{m_N} = \frac{\cos \theta \sin \psi + \sin \theta \sin \phi \cos \psi}{\sin \theta \cos \phi}.$$

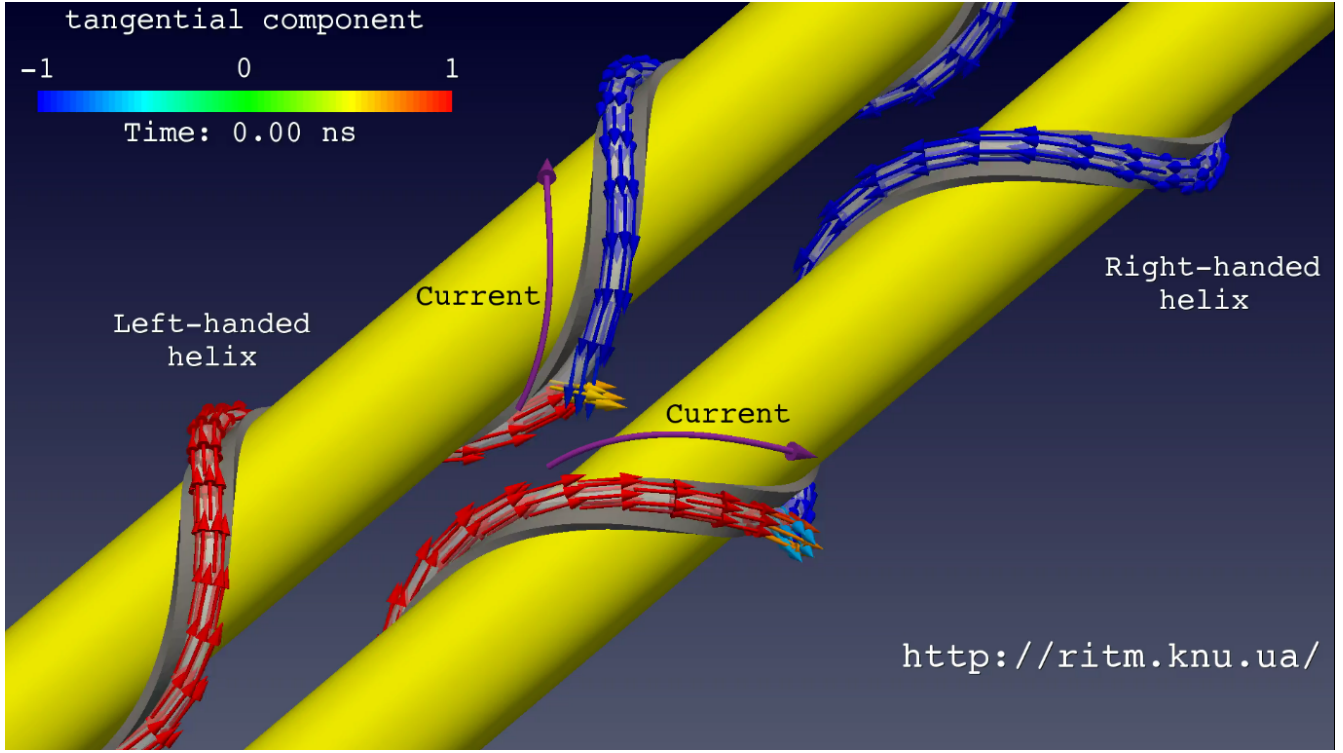
Comparison of the domain wall shapes in two above mentioned reference frames (magnetization components and angles) is shown in Fig. S1, obtained from SLaSi simulations,⁵ c. f. Fig. 4 of the manuscript, see Methods for details. Figures S1(a) and (b) clearly pronounce that the ground state is never strictly tangential one: the component m_B and, therefore, the angle $\tilde{\phi}$ are nonzero far from the domain wall. In the left and the right domains the magnetization states are $\tilde{\theta} = \psi$, $\tilde{\phi} = \pi/2 \pmod{2\pi}$ and $\tilde{\theta} = \pi - \psi$, $\tilde{\phi} = 3\pi/2 \pmod{2\pi}$ respectively. Inside the domain wall a bend of the the $\tilde{\phi}(u)$ profile appears. In the rotated reference frame domain wall structure significantly simplifies: $\phi(u)$ has a shape close to linear function and m_2, m_3 components becomes localized.

Figure S2 shows a comparison of domain wall structure for different values of quality factor $Q = K/2\pi M_s^2$: $Q = 0$ and $Q = 4$ in spin-lattice simulations with micromagnetic simulations and model where dipolar interaction is replaced by easy-tangential anisotropy only, see Methods for details.

3 Effective equations of the domain wall motion under the influence of Rashba torque

In order to derive effective equations of the domain wall motion we use generalized collective coordinate q - Φ approach⁶ based on the effective Lagrangian formalism. We start from the travelling wave Ansatz (see Eq. (6) of the manuscript):

$$\cos \theta^{\text{dw}}(u, \bar{t}) = -p \tanh \frac{u - q(\bar{t})}{\delta}, \quad \phi^{\text{dw}}(u, \bar{t}) = \Phi(\bar{t}) - \Upsilon [u - q(\bar{t})]. \quad (6)$$



Video S1. Motion of the head-to-head ($p = +1$) domain wall in helices with curvature $\varkappa = 0.1$ and torsion $\sigma = \pm 0.1$ under the action of the Rashba field $h = 0.02$.

One can derive the effective Lagrangian of the system by inserting this Ansatz into the full Lagrangian (S6), and calculating the integral over the dimensionless coordinate u . Then the effective Lagrangian, normalized by KSl reads $L^{\text{eff}} = G^{\text{eff}} - E^{\text{eff}}$ with effective gyroscopical term $G^{\text{eff}} = 2p\Phi\dot{q}$ and the effective energy, cf. Eq. (10) of the manuscript:

$$E^{\text{eff}} = \frac{2}{\delta} + \delta [2\mathcal{K}_1 + 2\Upsilon^2 + \mathcal{K}_2(1 + \mathcal{C}_1 \cos 2\Phi)] - 2\delta\mathcal{D}_1\Upsilon + p\mathcal{C}_2\mathcal{D}_2 \cos \Phi - 4phq \sin \psi,$$

$$\mathcal{C}_1 = \frac{\pi\delta\Upsilon}{\sinh(\pi\delta\Upsilon)}, \quad \mathcal{C}_2 = \frac{\pi(1 + \delta^2\Upsilon^2)}{\cosh(\pi\delta\Upsilon/2)}.$$

In the same way one can derive an effective dissipative function

$$F^{\text{eff}} = \eta \left[\frac{\dot{q}^2}{\delta} + \delta (\dot{\Phi} + \Upsilon\dot{q})^2 \right].$$

From the Euler-Lagrange-Rayleigh equations (11) for the set of variables $X_i = \{q, \Phi\}$ we obtain finally

$$\dot{\Phi}(p + \eta\delta\Upsilon) + \frac{\eta}{\delta}\dot{q}(1 + \delta^2\Upsilon^2) = 2ph \sin \psi, \quad \eta\delta\dot{\Phi} - \dot{q}(p - \eta\delta\Upsilon) = \mathcal{C}_1\mathcal{K}_2\delta \sin 2\Phi + \frac{p}{2}\mathcal{C}_2\mathcal{D}_2 \sin \Phi. \quad (\text{S8})$$

The effective equations of motion (S8) provide the domain wall motion with the finite velocity (see Eq. (7) of the manuscript):

$$v \equiv \frac{dq}{d\bar{t}}(\bar{t} \rightarrow \infty) = \frac{2ph\delta}{\eta} \cdot \frac{\sin \psi}{1 + \delta^2\Upsilon^2}. \quad (7)$$

The motion of domain walls in helices with different chiralities is illustrated by Supplementary Video S1.

The stationary phase $\Phi = \text{const}$ can be found from the equation:

$$2\mathcal{C}_1\mathcal{K}_2\delta \sin 2\Phi + p\mathcal{C}_2\mathcal{D}_2 \sin \Phi = -\frac{4ph\delta \sin \psi}{\eta(1 + \delta^2\Upsilon^2)}(p - \eta\delta\Upsilon).$$

In the case $\varkappa, |\sigma| \ll 1$, one gets

$$\Phi \approx \Phi_0 + \frac{2h\sigma}{\pi\eta}.$$

References

1. Sheka, D. D., Kravchuk, V. P. & Gaididei, Y. Curvature effects in statics and dynamics of low dimensional magnets. *J. Phys. A: Math. Theor.* **48**, 125202; DOI:10.1088/1751-8113/48/12/125202 (2015).
2. Slastikov, V. V. & Sonnenberg, C. Reduced models for ferromagnetic nanowires. *IMA J Appl Math* **77**, 220–235; DOI:10.1093/imamat/hxr019 (2012).
3. Sheka, D. D., Kravchuk, V. P., Yershov, K. V. & Gaididei, Y. Torsion-induced effects in magnetic nanowires. *Phys. Rev. B* **92**, 054417; DOI:10.1103/PhysRevB.92.054417 (2015).
4. Yershov, K. V., Kravchuk, V. P., Sheka, D. D. & Gaididei, Y. Curvature-induced domain wall pinning. *Phys. Rev. B* **92**, 104412; DOI:10.1103/PhysRevB.92.104412 (2015).
5. SLasi spin–lattice simulations package. URL <http://slasi.knu.ua> (Date of access:11/02/2016).
6. Kravchuk, V. P. Influence of Dzialoshinskii–Moriya interaction on static and dynamic properties of a transverse domain wall. *J. Magn. Magn. Mater.* **367**, 9; DOI:10.1016/j.jmmm.2014.04.073 (2014).